

## METHOD OF HORIZONTAL MAGNETOVARIAIONAL SOUNDING: TECHNIQUES AND APPLICATION IN THE EMTESZ-POMERANIA PROJECT

Varentsov Iv.M.<sup>1</sup> and EMTESZ-Pomerania Working Group<sup>2</sup>

<sup>1</sup>Geoelectromagnetic Research Centre, Institute of Physics of the Earth,  
Russian Academy of Sciences; Troitsk, Moscow Region, Russia; e-mail: igemil@mail.transit.ru;

<sup>2</sup>Listed in (Brasse et al., 2006)

### 1. Introduction

The horizontal magnetic inter-station operator  $\widehat{M}$  (horizontal magnetic tensor) describes in the frequency domain the linear relation between the horizontal magnetic field  $\mathbf{H}_h$  at two sites, the field site and the base,  $\mathbf{H}_h(\mathbf{r}) = \widehat{M}(\mathbf{r}, \mathbf{r}')\mathbf{H}_h(\mathbf{r}')$ . The anomalous operator,  $\widehat{M}^a = \widehat{M} - \widehat{I}$ , where  $\widehat{I}$  is a unit tensor, gives the “perturbation” linear relation:  $\mathbf{H}_h(\mathbf{r}) - \mathbf{H}_h(\mathbf{r}') = \widehat{M}^a(\mathbf{r}, \mathbf{r}')\mathbf{H}_h(\mathbf{r}')$ .

There are at least three general reasons to consider the  $\widehat{M}$  operator as an important part of the transfer function (TF) data set to be estimated and further interpreted in the simultaneous arrays of electromagnetic (EM) soundings. First, it looks free from hazardous galvanic distortions. Second, it can be reliably estimated in a broad period range sufficiently wider at long periods than that for the tipper. Third, it is reliably estimated at sites above centres of conducting anomalies, where tipper’s estimates are small in the amplitude and thus unstable.

A long tradition of using this response in EM studies starts from the monographs of Schmucker (1970) and Berdichevsky and Zhdanov (1984). Recent array studies brought a new quality of such estimates (Soyer, Brasse, 2001; Pajunpaa et al., 2002; Varentsov et al., 2003; Varentsov, Sokolova, 2003). However, the effective use of horizontal magnetic inter-station responses requires the development of techniques for their reliable multi-site estimation in spite of strong cultural noise and source distortions; base-to-base recalculation for the integration of data from several campaigns; rotational invariant analysis; separation of internal part, modelling and, finally, inversion. A progress in these directions was strongly motivated by the newest EM array sounding in Polish-German Pomerania (the EMTESZ-Pomerania Project) for the geoelectrical study of the lithosphere in the Trans European Suture Zone (TESZ).

The EM experiment held in 2001-5 in Polish-German Pomerania (EMTESZ-Pomerania WG, 2004; Brasse et al., 2006; Varentsov et al., 2005; etc.) gave a challenge to analyze horizontal magnetic inter-station responses together with other EM field transfer functions at a dense array located far away from the source inhomogeneities. About a hundred of simultaneous geomagnetic sites was observed there (Fig. 1) during several field campaigns with few repeated field bases and extra observatory references; and huge anomalies in  $\widehat{M}$  responses (up to 100% in the amplitude) have been traced within the TESZ. These soundings were concentrated along two deep seismic profiles (Guterch et al., 1999) passing the area from SW to NE, namely, P2 (southern) and LT-7 (northern), and along a new profile MT-5 across the Baltic Sea coast (Jozwiak, Neska, 2005).

The simultaneous soundings were performed in groups of 15-20 instruments with field bases at sites P8 (profile P2), G7 (profile LT-7) and P55 (profile MT-5). Observations at each site were held for few (1-6) weeks of proper recordings with 1-2 s sampling. Few sites were recorded with two different instruments for the control of their calibration and operational stability. The nearest geomagnetic observatory in Hel (HLP) was used as an extra stationary base, and two other observatories (BEL and NGK) stayed in reserve. Two of these bases, P8 and HLP, are connected with almost a unit  $\hat{M}$  tensor and seem to be located far enough from strong geoelectric anomalies. The base P8 was selected as a final reference for the presentation of the whole data array as the “quietest” in the sense of EM noise.

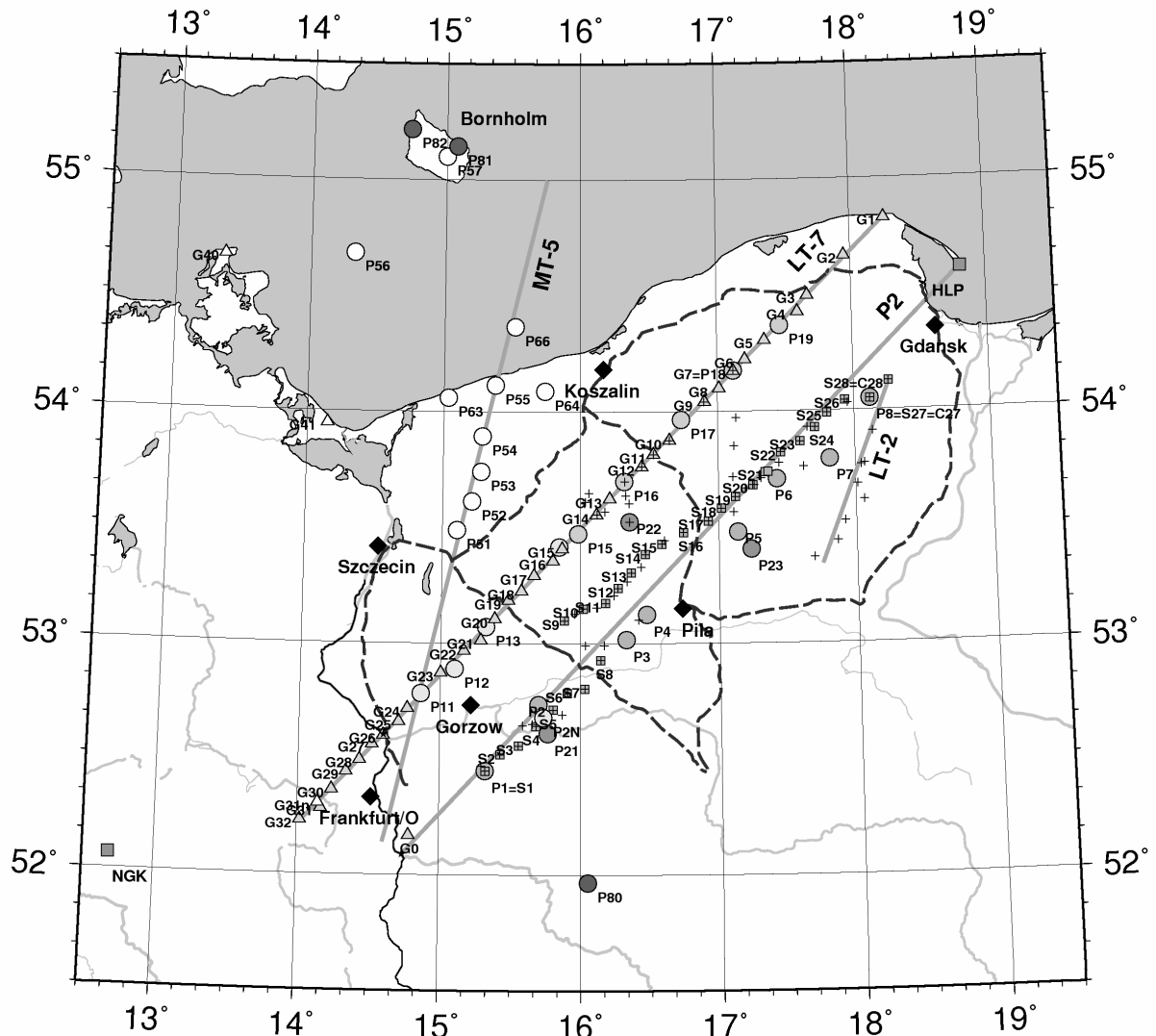


Figure 1. The EMTESZ-Pomerania array of EM soundings (Varentsov et al., 2005): Gxx (triangles) – German, Pyy (circles) – Polish, Szz (squares) - Swedish LMT sites, crosses – Czech, German and Swedish audio-MT sites; NGK and HLP (boxes) – geomagnetic observatories; dashed lines – DC railways.

The paper starts with a brief discussion of the data processing problems for the horizontal magnetic tensor and with a presentation of its primary estimates along Pomeranian profiles P2 and LT-7, then I consider rotational invariants of these data, further discuss the accuracy and temporal stability problems for this operator, and, finally, present first results in the inversion of the horizontal magnetic responses for the synthetic data set and for the Pomeranian data.

## 2. Estimation of the horizontal magnetic tensor

The estimation of the horizontal magnetic inter-station operator is discussed within our general data processing approach presented in (Varentsov et al., 2003, 2005; Sokolova, Varentsov, 2005). A two-site estimation scheme with a specific MC-sorting was applied within the EMTEZ-Pomerania experiment, giving reliable results in spite of strong EM noise influence (Sokolova, Varentsov, 2005). Several sites with repeated observations (P8, P55 and G7) were used as bases in the initial estimation.

Fig. 2 demonstrates the period dependence of main (diagonal) tensor components at two sufficiently anomalous sites at the LT-7 profile, namely, G10 and G16 (Fig. 1). It is possible to observe at this figure both the final results and the set of intermediate estimates obtained by the stacking of preliminary sorted partial estimates within time windows of different length further subjected to a multi-window robust averaging (Sokolova, Varentsov, 2005). The  $xx$ -amplitude at G10 doubles the unit normal level at periods around 1000 s, the same component at G16 raises up to 1.4 at longer periods around 3000 s. These amplitude maxima correspond well to zeros of the related phase components. The stability of all shown responses estimated in different time windows is obviously traced for periods at least within the range of 100-30000 s.

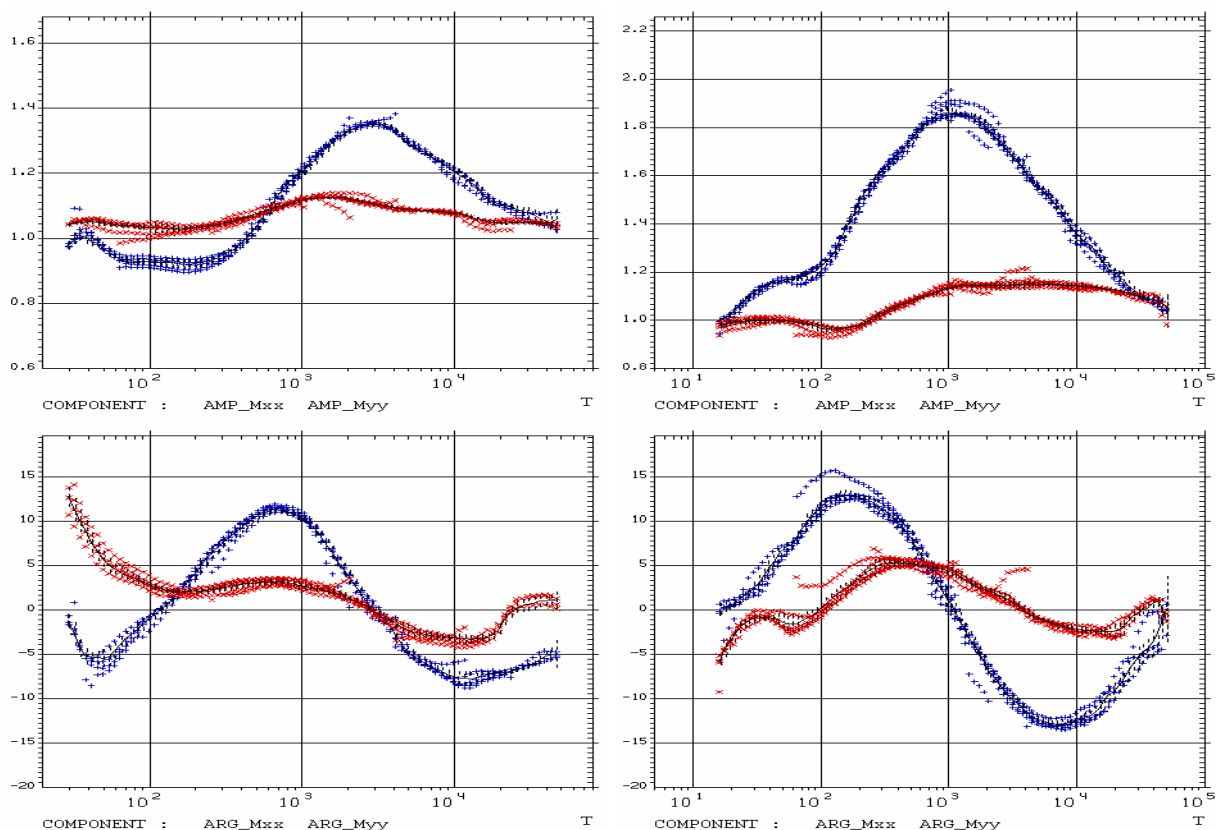


Figure 2. The horizontal magnetic tensor estimates (relative to site P8, amplitudes of main components at top panels and their phases at bottom ones) at sites G16 (left) and G10 (right) at the profile LT-7, which result from the multi-window averaging: “clouds” of crosses outline the whole set of the averaged data, solid lines with bars show final results.

A disturbing problem in the estimation of the horizontal magnetic tensor may be the synchronization of records from different types of instruments, sometimes operating at different sample rates. The analysis of the square determinant phase is the most helpful for its

solution. The hyperbolic approximation of this phase at shortest periods reliably reveals the time lag, which can be further accounted analytically for all the periods. Fig. 3 gives an example of such correction. In fact, the processed data at site S13 (Fig. 1) are initially sampled at 1 s rate, while at P8 they are resampled from 2 s records.

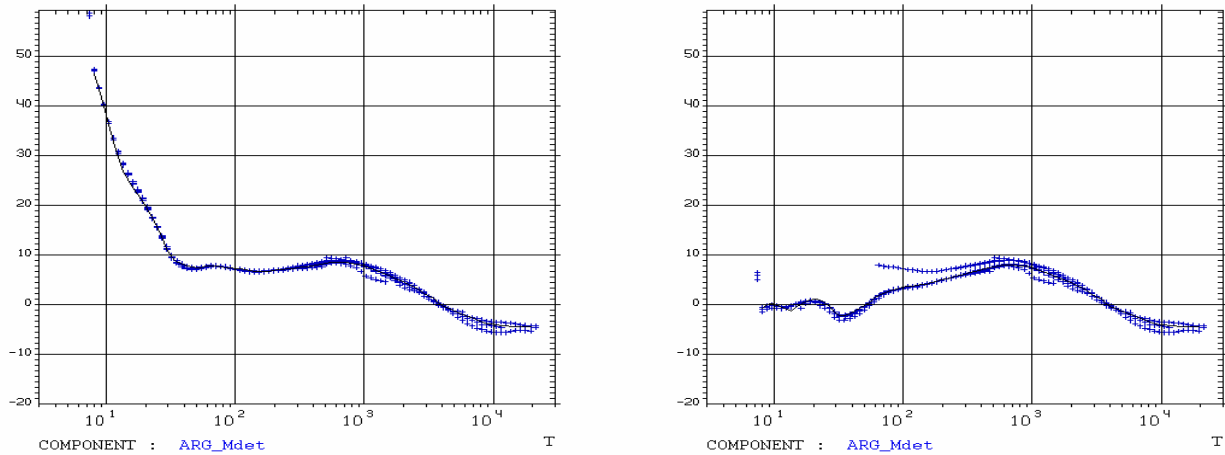


Figure 3. The time lag correction for operator  $\widehat{M}(S13, P8)$ : the initial determinant phase (left) and the phase corrected for a lag of 1 s (right).

Fig. 4 demonstrates pseudo sections of all amplitude and main phase tensor components along the two Pomeranian profiles. The major anomalies are traced in  $xx$ - and  $yx$ -components. The amplitude anomalies reach 100% level and the phase ones exceed 10 degrees.

### 3. Rotational invariants of the horizontal magnetic tensor

The simplest rotational invariant of the horizontal magnetic tensor is its square determinate, already considered in the analysis of a synchronization problem. The rotation procedure for this operator to a common coordinate frame generally depends on two clock-wise rotation angles  $\alpha$ ,  $\beta$ , relative to the observation frames at a field and at a base, correspondingly:

$$\widehat{M}(\alpha, \beta) = \widehat{R}(\alpha)\widehat{M}(0,0)\widehat{R}(-\beta), \quad \widehat{R}(\varphi) = \begin{bmatrix} \cos(\varphi) & \sin(\varphi) \\ -\sin(\varphi) & \cos(\varphi) \end{bmatrix}.$$

The extension of a classic Swift's formalism, searching an azimuth minimizing the amplitude of the tensor's off-diagonal elements in the course of rotation within a common coordinate system, yields:

$$\begin{aligned} & |M_{xy}(\alpha, \alpha)|^2 + |M_{yx}(\alpha, \alpha)|^2 = \\ & = 2 \left\{ |M_2(0,0)|^2 + |M_1(0,0)|^2 \cos^2 2\alpha + |M_3(0,0)|^2 \sin^2 2\alpha - \right. \\ & \left. - \operatorname{Re}[M_1(0,0)M_3^*(0,0)] \sin 4\alpha \right\} = \min_{\alpha} \end{aligned}$$

where

$$\begin{aligned} M_1 &= (M_{xy} + M_{yx})/2, \quad M_2 = (M_{xy} - M_{yx})/2, \\ M_3 &= (M_{xx} - M_{yy})/2, \quad M_4 = (M_{xx} + M_{yy})/2. \end{aligned}$$

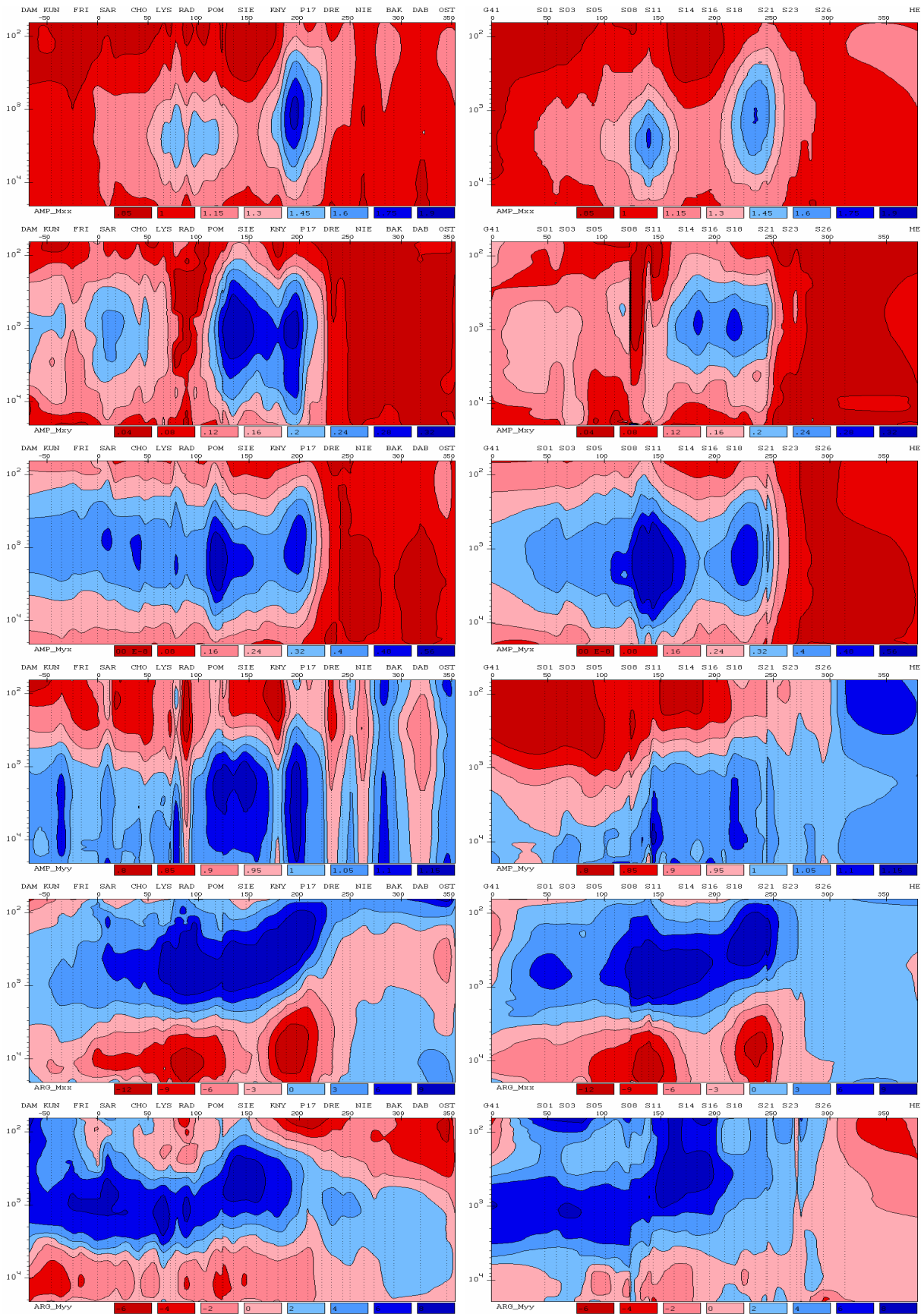


Figure 4. Pseudo sections of the horizontal magnetic tensor components (relative to P8 base) along two profiles, LT-7 (left) and P2 (right); from top to bottom:  $xx$ -,  $xy$ -,  $yx$ - and  $yy$ -amplitudes,  $xx$ - and  $yy$ -phases.

This minimization yields the principle direction azimuths defined by an angle  $\gamma_M$ :

$$\gamma_M = \frac{1}{4} \arctg \frac{2 \operatorname{Re}(M_1 M_3^*)}{|M_3|^2 - |M_1|^2},$$

which is obtained in a sequence with a  $\pi/2$  period. It is necessary to compare the amplitudes  $|M_{xx}(\gamma_M, \gamma_M)|$  and  $|M_{xx}(\gamma_M + \pi/2, \gamma_M + \pi/2)|$  to select proper maximal and minimal azimuths from this sequence. The maximal and minimal amplitudes and phases are naturally obtained with a rotation to correspondent maximal and minimal azimuths. Finally, the horizontal magnetic skew-parameter takes the form:  $skew_M = |M_2|/|M_4|$ .

Fig. 5 presents at both Pomeranian profiles pseudo sections of different invariants of the total horizontal magnetic operator. The maximal amplitude looks simple, smooth but informative: two prominent (up to 100%) positive deep anomalies appear at the edges of the TESZ with a maximum at 1000-2000 s periods and indicate two strong quasi-2D current systems in the crust; the amplitude decrease is observed at short periods pointing at the resistive sedimentary centre of the TESZ; a high homogeneity of the data is traced at the Precambrian Craton (on the right) and more inhomogeneities are seen at the less consolidated Palaeozoic Platform (on the left). The maximal phase outlines a general subhorizontal stretch of an area with excessive conductivity in the middle of the TESZ with a clear SW deepening. The overall horizontal magnetic skew is quite low but increases in the TESZ centre and at the Palaeozoic Platform.

Similar invariants for the anomalous tensor  $\widehat{M}^a$  display anomalous properties of the horizontal magnetic tensor and specify "perturbation" vectors or ellipses (Schmucker, 1970; Pajunpaa et al., 2002; Varentsov et al., 2005; Brasse et al., 2006) complementing the induction vectors in the magnetovariational (MV) imaging of geoelectric structures. An obvious interpretation of perturbation ellipses is possible when the geoelectric structure well-around the base site can be considered as 1D. In this case (Varentsov et al., 2005) ellipses are almost zero within areas of quasi-1D structure close to that at the base site, take a circular form above quasi-1D structures different from the structure at the base site, stretch as a bar around 2D structures and keep a general ellipse form in the presence of 3D effects.

Fig. 6 displays long-period extreme amplitude ellipses of the anomalous horizontal magnetic operators over the subsurface conductance map (EMTESZ-Pomerania WG, 2004; Jozwiak, Ernst, 2005). These ellipses at the Craton are almost "zero" indicating its electrical homogeneity at the depth. Such an area is wide enough (of a hundred-km scale) to justify a proper selection of the common base site P8 (Fig. 1).

The horizontal magnetic strike appears to be quite stable around  $60^\circ\text{NW}$  with the greatest variance at the edges of profiles. A good agreement is achieved in the EMTESZ-Pomerania experiment between invariant azimuths of the horizontal magnetic tensor and galvanically undistorted principal directions of the impedance phase tensor (Varentsov et al., 2005). This agreement confirms a presence of a deep conducting 2D structure striking at  $\sim 60^\circ\text{NW}$ . The deep strike direction differs from  $\sim 45^\circ\text{NW}$  strike of principle subsurface sedimentary structures, clearly outlined in the presented conductance map. The view of the horizontal inter-station magnetic response within the whole EMTESZ-Pomerania array (Varentsov et al., 2005) proves its 2D structure in the vicinity of profiles P2 and LT-7.

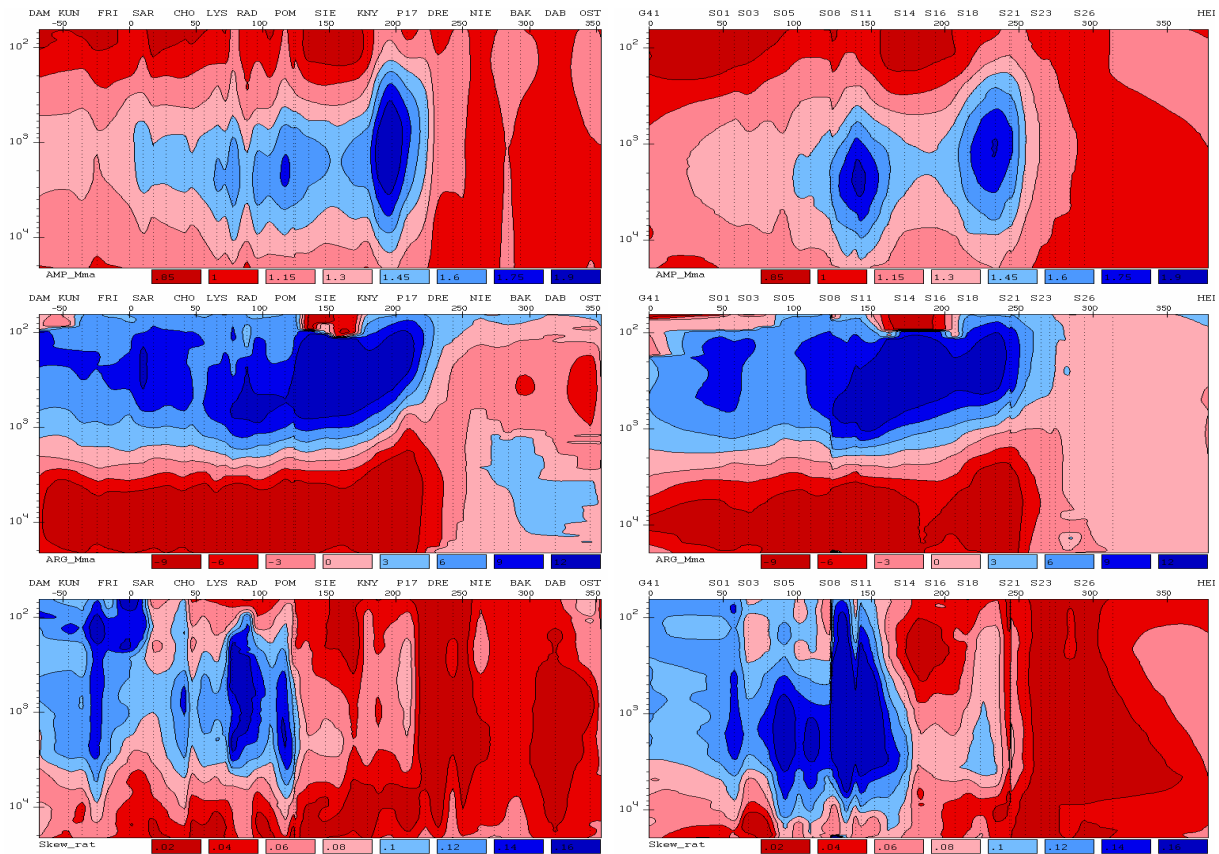


Figure 5. Pseudo sections of rotational invariants for the horizontal magnetic tensor (relative to P8 base site) along two profiles, LT-7 (left) and P2 (right); from top to bottom: maximal amplitude, maximal phase and the  $skew_M$  parameter.

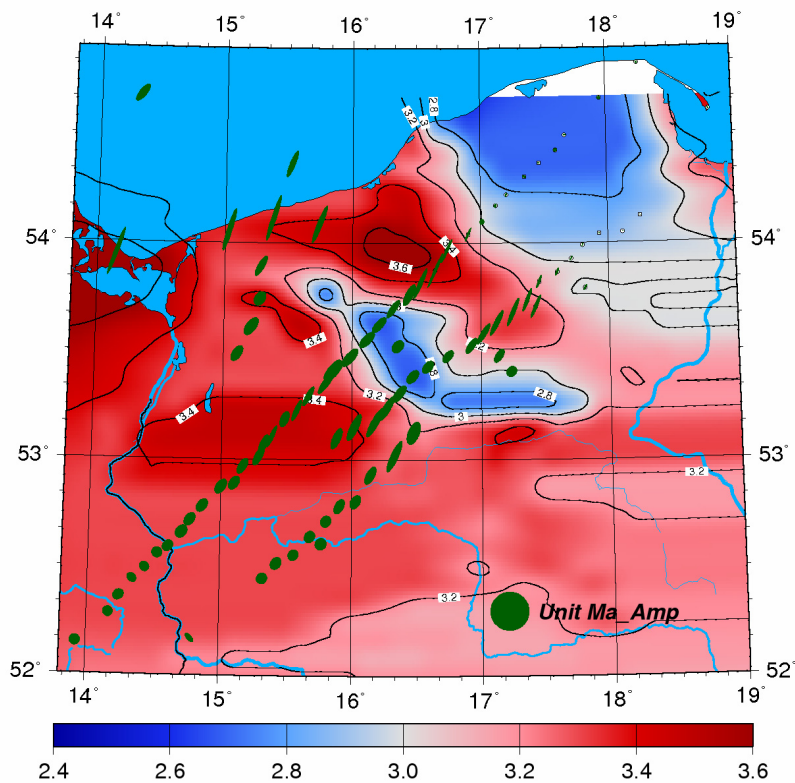


Figure 6. Extreme amplitude ellipses of the anomalous horizontal magnetic operator (relative to P8 base site) over the subsurface conductance map (in a  $\log_{10}$ -scale).

#### 4. Accuracy control and temporal stability of the horizontal magnetic tensor

The quality of  $\widehat{M}$  tensor data is controlled with multiple bases and repeated observations to compare the fit of direct  $\widehat{M}(\mathbf{r}_a, \mathbf{r}_b)$  and “transitive”  $\widehat{M}(\mathbf{r}_a, \mathbf{r}_b / \mathbf{r}_c) = \widehat{M}(\mathbf{r}_a, \mathbf{r}_c) \widehat{M}(\mathbf{r}_c, \mathbf{r}_b)$  calculations and to justify the temporal stability of responses (Varentsov et al., 2003; Varentsov, Sokolova, 2003). Fig. 7 compares direct and transitive data at two sites at the profile LT-7. The fit at site P15 is excellent and the transitive estimate at site G9 (with a relatively short record simultaneous with P8 for the direct estimate) looks preferable.

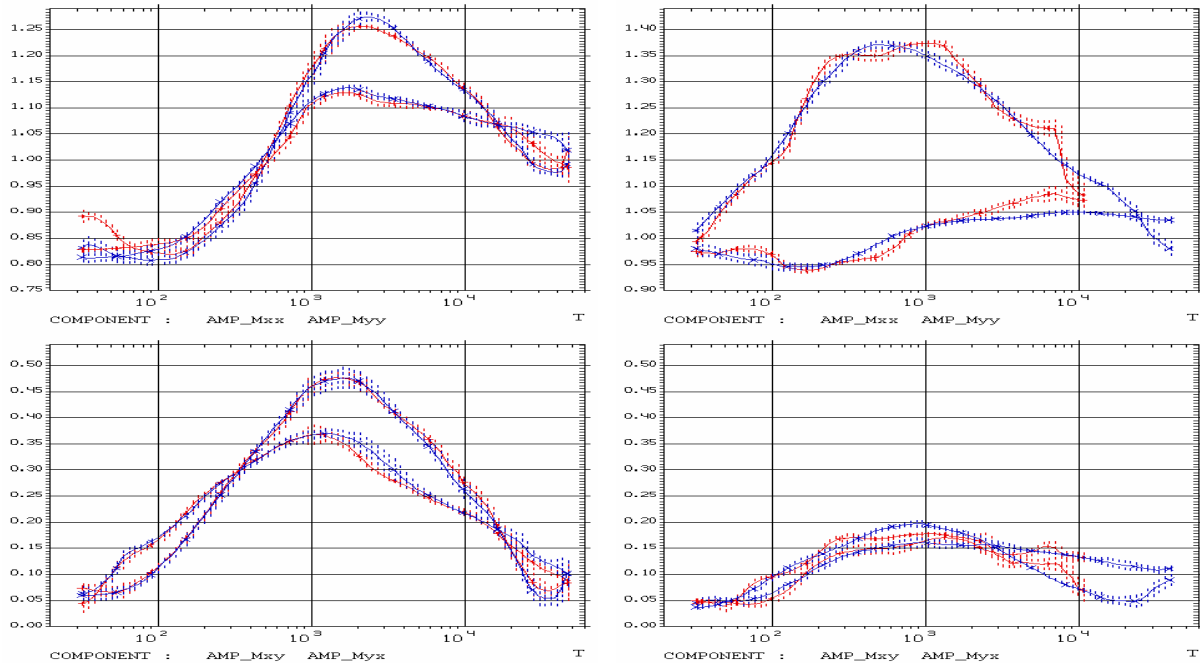


Figure 7. Transitive (via site G7, blue) and direct (red) period-dependent estimates for  $\widehat{M}(P15, P8)$  and  $\widehat{M}(G9, P8)$  operators (left and right panels, respectively) at the profile LT-7;  $xx$ - and  $yy$ -amplitudes at top panels,  $xy$ - and  $yx$ -amplitudes at bottom ones.

Fig. 10 presents the convergence of the repeated  $\widehat{M}(BEL, HLP)$  extreme amplitude and maximal azimuth estimates, which link two adjacent geomagnetic observatories. Temporal deviations of maximal and minimal amplitudes lie at a few percent level of the estimation error bars and are much smaller than the amplitude anomaly in the TESZ (Fig. 5). The azimuth response has a prominent stability at periods below 2 hours. The observed stability justifies a reliable recalculation of operators  $\widehat{M}$  in the process of the reduction of estimates obtained for separate simultaneous clusters to the common base.

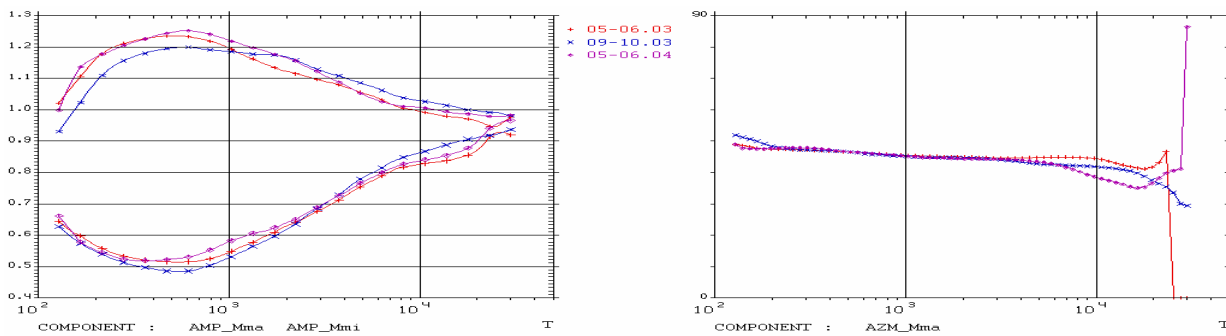


Figure 8. Repeated  $\widehat{M}(BEL, HLP)$  estimates, maximal and minimal amplitudes (left) and maximal azimuth (right), for observation intervals (months.year) given in the legend.



## 5. Two-dimensional inversion of the horizontal magnetic responses

The tools to invert horizontal magnetic “profiles” (separately or combined with other responses) in 2D models are ready (Varentsov, 2002, 2005a,b). Inversion of synthetic data sets of the COPROD-2S international project (Varentsov, 1998) gives an example of encouraging resolution extracted both from single horizontal magnetic responses and from multi-component data ensembles with their inclusion (Varentsov, 2005a,b). Fig. 9 compares inversion solutions for the COPROD-2S1 data set in the case of a complicated geoelectric model containing numerous closely located conducting anomalies. The inversion model for the horizontal magnetic data in this figure looks even preferable in the resolution of the deepest targets in comparison with solutions for the impedance and tipper data.

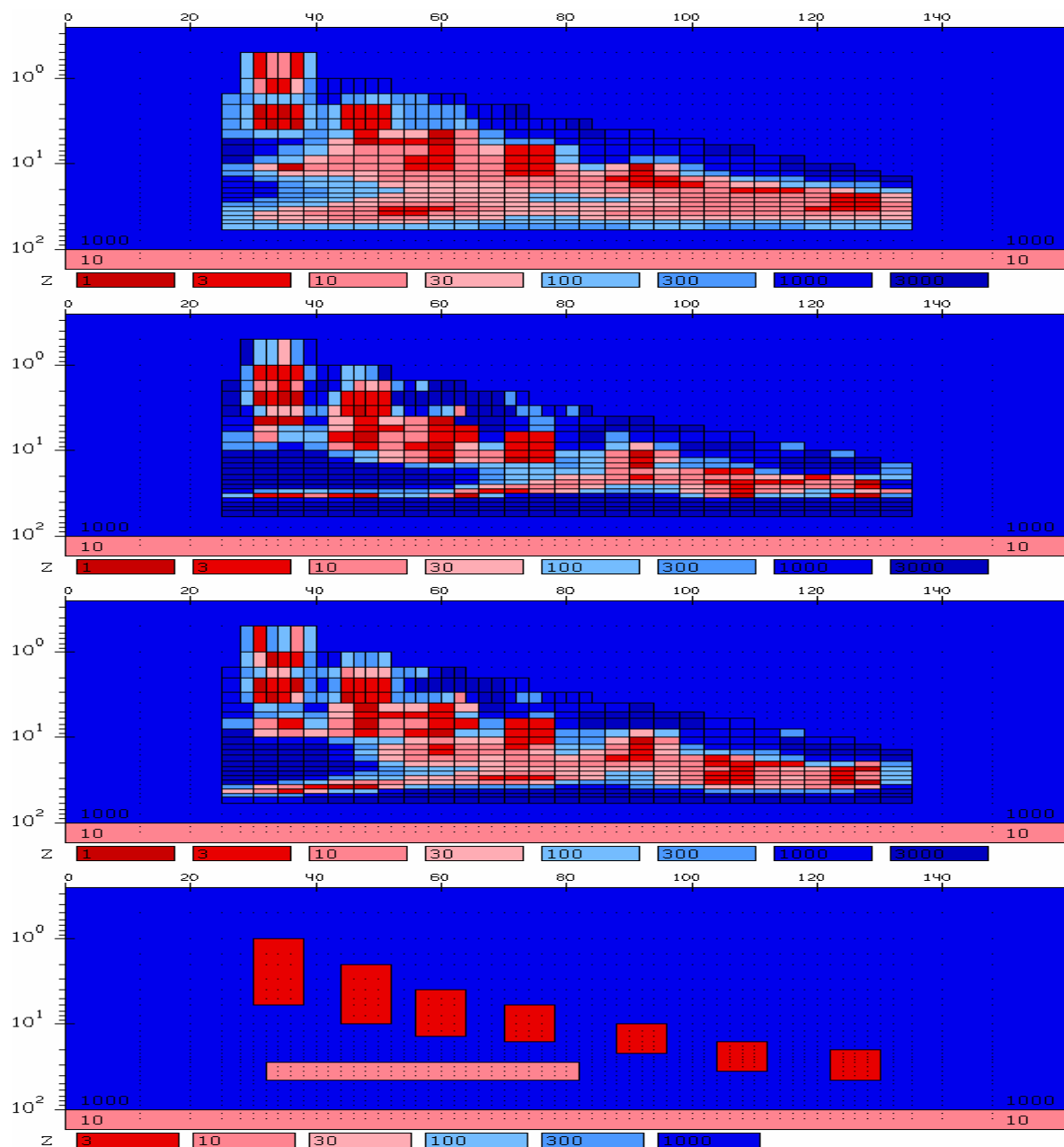


Figure 9. Two-dimensional inversion of the COPROD-2S1 synthetic data set, from top to bottom: for the E-polarization impedance (apparent resistivity and phase), for the tipper (Re,Im), for the horizontal magnetic field (Mod,Phase); the true model is in the bottom.

First results in the inversion of the horizontal magnetic responses in the EMTESZ-Pomerania project are also looking encouraging. The amplitude and phase of  $M_{xx}$  data (after 30°NE rotation of the original operators) were inverted in 2D along P2 and LT-7 profiles. The inverted data (Fig. 10) look quite close to maximal amplitude and phase responses in Fig. 5. The anomalous model structure was scanned in 3 windows (sedimentary, crustal and upper mantle), which cover the whole TESZ section and almost the whole observation interval. The parameterization scheme with the correlated cell resistivities was applied within these windows (Varentsov, 2002, 2005a). The resulting parameters were optimized together with the resistivities of the normal geoelectric structure. The robust inversion iterations at the both profiles were terminated at the RMS level of  $\sim 2.5$  with absolute amplitude misfit norms being below 0.05 and absolute phase misfit norms being below 1.6°.

Fig. 10 demonstrates resulting inversion models at both profiles and the data fit pseudo sections. These models, in spite of their preliminary character, have a number of stable common features. The crustal anomalous conductivity is concentrated in the central part of the TESZ in the horizontal interval of about 120 km and the depth range of 10-30 km, which is generally dipping from the edge of the Precambrian Craton towards the Palaeozoic Platform. It has several local extrema with resistivity lower than 1  $\Omega\cdot\text{m}$ . The sedimentary structure exhibits two conducting troughs at the margins of the TESZ with the conductance at the level of 1000 S and a central resistive part. The normal section structures also correlate quite well. The crustal resistivity of the Craton is higher than on the Palaeozoic Platform. The upper mantle structure at the Craton seems to be normal, in the TESZ it even has the increased resistivity, while at the Palaeozoic Platform the resistivity in the depth range of 100-200 km decreases to the level of 25  $\Omega\cdot\text{m}$ , which is quite typical for the “electrical asthenosphere”.

The listed geoelectric features of the TESZ can be resolved in more details and with a greater stability in the inversion of multi-component quasi-2D data ensembles combining the most reliable MT/MV data components and accounting for 3D distortions available (Varentsov et al., 2005). The demonstrated data fit may be improved for the same data at finer grids. The inversion studies in the EMTESZ-Pomerania project are still on the way. Nevertheless, even the presented preliminary inversion results demonstrate quite obviously the rich interpretation resources for the deep model resolution contained in the horizontal magnetic inter-station responses.

## 6. Conclusions

A number of techniques for the whole range of tasks from the estimation of the horizontal magnetic inter-station responses till their inversion is presented and jointly applied to the data of the EMTESZ-Pomerania array sounding. An important experience is shown in the overcoming of strict EM noise effects in the data processing and in the invariant analysis of the results. Quite accurate and dense quasi-2D horizontal magnetic data sets along two profiles with several bright anomalies of the crustal nature are selected for further interpretation, both separate and joint with other MT/MV responses. First results of the horizontal magnetic data 2D inversion along the EMTESZ-Pomerania profiles look very encouraging.

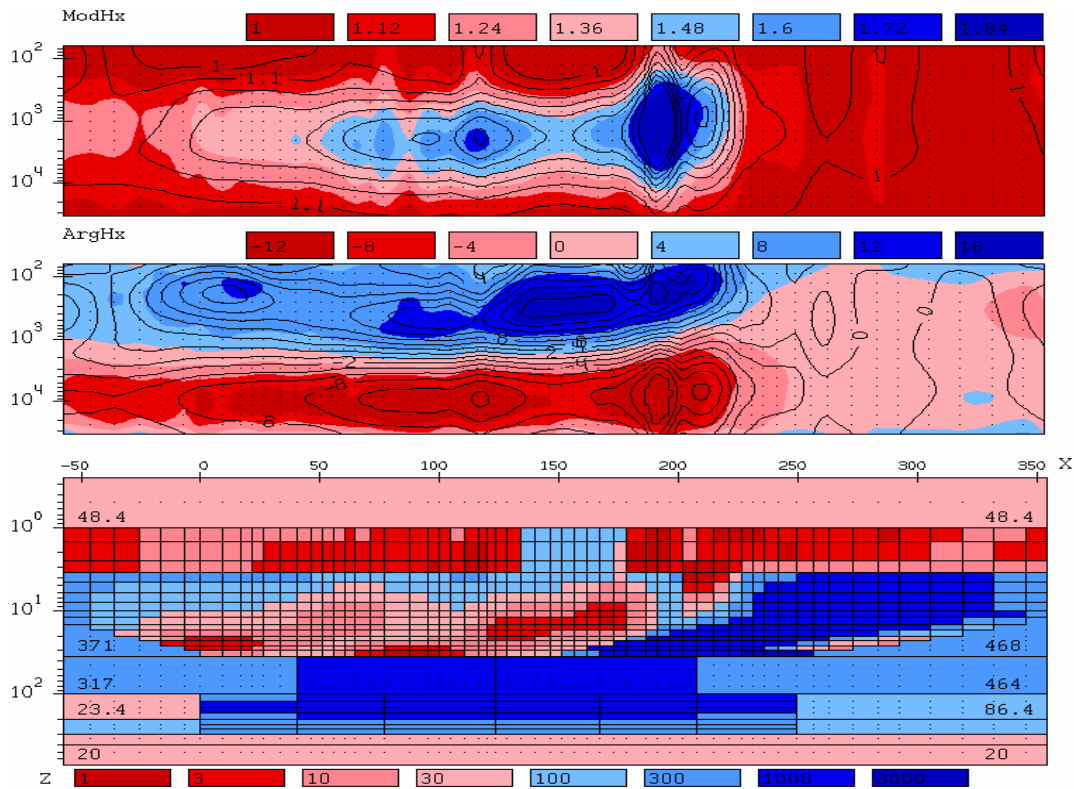


Figure 10a.  $M_{xx}$  data inversion at the profile LT-7, from top to bottom: data fit in pseudo sections for the amplitude and phase (the observed data are given in colours, the modelled data overlap them in black contour isolines) and the resulting 2D model (resistivity in  $\Omega\cdot\text{m}$ , the vertical scale is logarithmic, the horizontal axis origin is at Polish-German border).

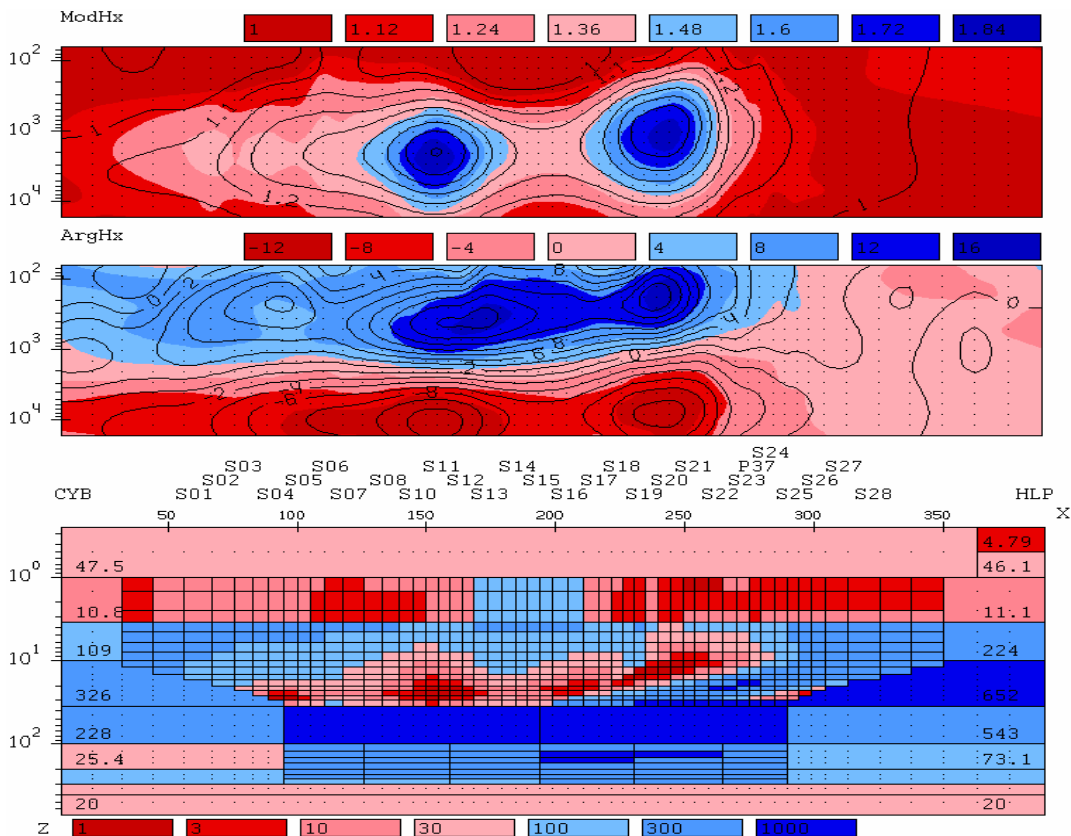


Figure 10b.  $M_{xx}$  data inversion at the profile P2, the legend is the same as in Fig. 10a.

## Acknowledgements

I would like to thank my colleagues in BEAR and EMTESZ-Pomerania Working Groups for a long-term cooperation in the analysis of geomagnetic inter-station responses, and M. Berdichevsky and U. Schmucker for valuable discussions. This work was supported by DFG-RFBR Grant 03-05-04002 and NATO Collaboration Linkage Grant EST.CLG.980126.

## References

- Berdichevsky, M.N., and M.S. Zhdanov, 1984. Advanced theory of deep geomagnetic sounding. Elsevier, Amsterdam - Oxford - New York – Tokyo, 408 p.
- Brasse, H., Cerv, V., Ernst, T., Jozwiak, W., Pedersen, L.B., Varentsov, Iv.M., and EMTESZ-Pomerania WG, 2006. Probing the electrical conductivity structure of the Trans-European Suture Zone. *Eos Trans. AGU* (Submitted).
- EMTESZ-Pomerania WG, presented by Varentsov, Iv.M., 2004. EMTESZ-Pomerania: an integrated EM sounding of the lithosphere in the Trans-European suture zone (NW Poland and NE Germany). XVII Workshop on EM Induction in the Earth (Abstracts). Hyderabad, India, 133-134.
- Guterch, A. et al., 1999. POLONAISE'97— International seismic experiment in Poland. *Tectonophysics*, **314**, 101–121.
- Jozwiak, W., and Ernst, T., 2005. Main conductivity anomalies in Poland in relation to geological structure. Study of geological structures containing well-conductive complexes in Poland, *Publ. Inst. Geophys. Pol. Acad. Sci., Warszawa*, C-95(386), 5-16.
- Jozwiak, W., and Neska, A., 2005. EM sounding in SW Baltic region: significant induction anomaly indicated by perturbation vectors. Study of geological structures containing well-conductive complexes in Poland, *Publ. Inst. Geophys. Pol. Acad. Sci., Warszawa*, C-95(386), 97-106.
- Pajunpaa, K., Lahti, I., and B. Olafsdottir, 2002, Crustal conductivity anomalies in central Sweden and SW Finland: *Geophys. J. Int.*, **150**, 695-705.
- Schmucker, U., 1970. Anomalies of geomagnetic variations in the SW United States. Univ. of California Press, Berkeley.
- Sokolova, E.Yu., Varentsov, Iv.M., and EMTESZ-Pomerania WG, 2005. RRMC technique fights highly coherent EM noise. This book.
- Soyer, W., and H. Brasse, 2001. A magneto-variation study in the central Andes of N Chile and SW Bolivia. *Geophys. Res. Let.*, **28**(15), 3023-3026.
- Varentsov Iv.M., 1998. The COPROD-2S project. WWW page, [http://user.transit.ru/~igemi/c\\_2s\\_p0.htm](http://user.transit.ru/~igemi/c_2s_p0.htm).
- Varentsov, Iv.M., 2002. A general approach to the magnetotelluric data inversion in a piecewise-continuous medium. *Izvestiya, Phys. Solid Earth*, **38**(11), 913-934.
- Varentsov, Iv.M., 2005a, Robust methods of joint inversion of MT/GDS data in the piecewise-continuous media. *Electromagnitnye issledovania zemnykh nedr* (Ed. Spichak V.V.). Nauchny Mir, Moscow, 54-75 (in Russian).

- Varentsov, Iv.M., 2005b. Arrays of simultaneous EM soundings: methods of construction and analysis. *Electromagnitnye issledovaniya zemnykh nedr* (Ed. Spichak V.V.), Nauchny Mir, Moscow, 143-156 (in Russian).
- Varentsov, Iv.M., and EMTESZ-Pomerania WG, 2004. The estimation and analysis of horizontal magnetic inter-station transfer functions in the EMTESZ-Pomerania project. XVIII Workshop on Electromagnetic Induction in the Earth (Abstracts), Hyderabad, India, 153-154.
- Varentsov, Iv.M., Sokolova, E.Yu., and BEAR WG, 2003. Diagnostics and suppression of auroral distortions in the transfer operators of the EM field in the BEAR experiment. *Izvestiya, Phys. Solid Earth*, **39**(4), 283-307.
- Varentsov, Iv.M., Sokolova, E.Yu., Martanus E.R., and EMTESZ-Pomerania WG, 2005. Array view on EM transfer functions in the EMTESZ-Pomerania project. Study of geological structures containing well-conductive complexes in Poland, *Publ. Inst. Geophys. Pol. Acad. Sci., Warszawa, C-95(386)*, 107-121.
- Varentsov, Iv.M., Sokolova, E.Yu., Martanus, E.R., Nalivayko, K.V., and BEAR WG, 2003. System of EM field transfer operators for the BEAR array of simultaneous soundings: methods and results. *Izvestiya, Phys. Solid Earth*, **39**(2), 118-148.